Circularly Polarized Phased Antenna Array with Pseudo-Conical Scanning with an Application for UAVs Unmanned Landing

Ivaylo Nachev
dept. Radio Communication and Video Technologies
Technical University of Sofia8
Sofia, Bulgaria
ivaylonachev@yahoo.com

Ilia G. Iliev
dept. Radio Communication and Video Technologies
Technical University of Sofia
Sofia, Bulgaria
igiliev@tu-sofia.bg

***Abstract*—This work shows the main requirements for a system for an unmanned landing of a flying vehicle using a pseudo-conical scanning method. The research work focuses on the system sensor - a circularly polarized phased antenna array with pseudo-conical scanning, for locating, intercepting and controlling the detected object - UAV. A functional model of the considered antenna system, with nine beam states, is created. Simulated and measured results are presented.**

Keywords— phased antenna array, scanning antenna, beamforming, phase shifting, radiation pattern, pseudo-conical scanning, autonomous flying vehicle, UAV's, drones, autonomic landing.

I. INTRODUCTION

Virial applications of UAVs to solving tasks of different nature are applicable. They can be used to automate and integrate new technologies with great accuracy in specific processes, such as defense purposes [1], search and assessment in areas of disaster, accidents, and environmental disasters [2], and monitoring of forests, agricultural crops agricultural activities [3], mapping, geodetic activities, rapid updating of topographic information in settlements [4], delivery of consignments [5] and etc. All these applications form the design requirements for UAVs, several of which are related to the systems for automatic vehicle tracking and landing. Most known landing methods for the unmanned landing of UAVs are based on: differential GPS systems [6], laser optical curtain [7], video systems, image recognition on the landing pad [8], and e.t.

Navigation methods with radio signal processing and, in particular, pseudo-conical scanning (PCS) have long been known for the imposition of the basic principles of navigation radars. They are widely used in automatic satellite docking, tracking satellites from terrestrial telecommunication stations, and tracking and navigating mobile objects [9].

- It is possible to track and navigate remote objects at greater distances from optical systems. The only limiting condition is the energy balance of the radio connection with the moving object;
- Satisfactory accuracy for navigation, guidance, and execution of the automatic landing process. Due to the nature of the PCS, it is interesting to note that the positioning accuracy increases with decreasing distance between the UAV and the landing pad;
- The landing pad dimensions should be commensurate with the UAV dimensions;
- Ability to work in bad weather, rain, snow, smoky areas, etc. Naturally, it depends on the selected operating frequency range and hence on the peculiarities of the propagation of electromagnetic waves;
- Possibility to landing on mobile platforms;
- Relatively low cost and easy implementation.

The multi-beam electromagnetic wave propagation significantly affects the accuracy, mainly in the presence of obstacles. The received signal power can fluctuate in 3-6dB range. That is one of method disadvantages related to the requirement for direct visibility between the moving object and a landing pad. The distribution model can then be interpreted as a Rice fading model. This effect can generally be minimized if the antenna array used for PCS has a low level of RP side lobes. Moreover, as the distance between the UAV and the landing pad decreases, the accuracy of positioning increases. In addition, the signal strength from the direct beam with direct visibility increases compared to those with reflected signals.

This paper considers the circularly polarized phased antenna array with a pseudo-conical scanning for implementation in an unmanned aerial vehicle (UAV) landing pad. The landing systems requirements and system sensor - PAA parameters are defined.

The described antenna has nine beam states, which are used to determine the location and UAV control that falls into coverage of the antenna - sensor range. Simulated and measured results of the synthesized antenna array are presented. The presented results prove the discussed PAA applicability for the UAV unmanned landing pad.

II. THE UAV LANDING PAD SENSOR REQIREMENTS

Sensor for the automatic landing system of a UAV is performed by a phased antenna array. This autonomous radio navigation system is used to determine the relative position of an object in space - Figure 1. The unmanned landing of UAVs on a site is performed as follows: UAV is directed to the landing site via its coordinates (using civil GPS systems). Once the UAV is positioned, the range of the sensor PAA with pseudo-conical scanning, the range of which is calculated to capture the object set at the appropriate GPS coordinates, and the algorithm for

978-1-6654-8212-7/22/$31.00 ©2022 IEEE

automatic landing begins. The algorithm must include the following main processes: determining the vehicle location in space relative to the coordinate system of the landing site; tracking, filtering, and directing to the center (the sensor center).

- Operating frequency 2400MHz - part of the free licensing ISM band, also frequency already used to control some types of UAVs;
- Linear polarized transmitting antenna mounted on the UAV board with a gain $G_{Atx} \leq 2dBi$;
- UAVs transmitter out power $P_t \approx 10\ dBi$;
- Receiving antenna implemented in the landing pad sensor with a gain $G_{Arx} \leq 4dBi$;
- The A_{rx} with 9 beam scanning states - $\theta_{scan} \approx 20^o$, are required to ensure sufficiently high accuracy of the sensor;
- The receiving part must measure the level of a UAV transmitted signal;
- Communication channel transmitting commands for UAV positioning above the landing pad, based on the signals measured by the receiving antenna;
- The vehicle location determination algorithm in space relative to the coordinate of the landing site; algorithm must following steps: tracking, filtering, command sending, and directing to the center of the coordinate system (the sensor center).

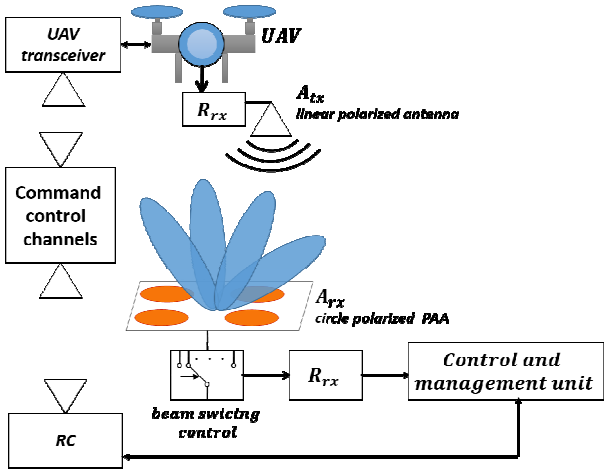

Fig. 1. Block diagram of the automatic landing of UAVs system

III. The Phased Antenna Array Design

To comply with all the requirements for a phased antenna array for integration in the UAVs unmanned landing, a circularly polarized array (construction type 2x2) in a planar realization is designed. This design allows a feed network's easy tunning to control the antenna beam on azimuth and elevation planes. Pre-positioned sensor relative to the ground requires the definition of ϕ and θ planes, respective to E and H planes.

An elementary PAA emitter - patch antenna chosen, designed in dielectric substrate with: ε_r= 4.75, tangδ=0.003, thickness h=1.5mm and operating frequency -fc= 2400MHz. To optimize antenna array design and manufacturing and reduce the influence of surface waves between elements in the array, a circularly polarization patch with a circle form - a resonator with a diameter: λg/2 or [10] is used:

$$D_{patch} = \frac{\lambda_g}{2} \quad (1)$$

where:

$$\lambda_g = \frac{\lambda}{\sqrt{\varepsilon_r}} = \frac{c}{f_c\sqrt{\varepsilon_r}} \quad (2)$$

From the patch antennas theory for obtaining a characteristic impedance of 50Ω, the excitation point is equal to a distance of $feedpoint \approx 0.5DPATCH$ from the center of the patch. Therefore circularly polar is obtained by adding a second feed point of 90º electrical length through the first. The phase of the second feed point can be commissioned with an expended patch feed network using hybrid devise or dephasing networks [10, 11].

Using the presented equations, the synthesized patch dimensions are: D_{patch}=28.67mm and $feedpoint$=7.16mm. After optimization (using openEMS using FDTD method) the optimal antenna dimensions are achieve were reduced to D_{patch}=28.67mm and $feedpoint$=7.16 mm.

The next step is implementing the optimized patch in a phased antenna array. Theoretically, the distance between PAA elements is within 0.4λ ÷ 0.7λ [12, 13]. A toolbox of Matlab was used to find the optimal distance between the antenna array radiators and the appropriate phases for the element's current excitation in scanning mode. The tool allows the simulation of different configurations of antenna arrays using stimulation equations The array factor for the MxN array for the x-y plane is given by [14, 15]:

$$AF(\theta,\phi) = \sum_{m=1}^{M}\sum_{n=1}^{N} w_{mn} e^{j[(m-1)\psi_x + (n+1)\psi_y]} \quad (3)$$

Where:

$$\psi_x = kd_x sin\theta cos\phi \quad (4)$$

$$\psi_y = kd_y sin\theta cos\phi \quad (5)$$

Where the d_x and d_y is a distance between two adjacent radiation elements along the axis x and y, w_{mn} are elements' current excitation.

Settings the software with $AF(\theta,\phi) \approx 20^o$ values in beam deviation in scanning mode, the current excitation phase values were found at both points w_n=w_m=90º, and optimal distances between the array elements is d_x=d_y=0.5λ. The gain of the antenna array is obtained G_{Arx}=7.5dBi, which fully meets requirements discussed in the previous section.

The next step in the PAA design is to provide circular polarization in the scanning mode. There are used two main techniques for performing circularly polarized antenna arrays. An approach allowed a circularly polarized antenna array with linearly polarized elements [16]. This technique proposed circle polarization in scan mode, but high gain is not maintained in different beam states. The technique for circular polarization in an antenna array is used, where the current phase excitation in all patches is equalized. This is also necessary due to the use of a -3dB bridge for the circular polarization of each individual element. When changing phases to one of the patches, to maintain the circular polarization, their moment phases must also be equalized to obtain a circular polarization in beam scanning mode. Therefore, for some of the excitation points for individual elements, an additional phase of electrical length

is added - 180º, in this case. Another feature of the design of PAA for navigation purposes is symmetry between the antenna excitation points. Thus, symmetry is maintained between the centers of opposite states of the RP in scanning mode. A simulation model of the circularly polarized PAA is shown in Figure 2. The figure also shows the current excitation of the antenna array and the moment phases in each of the elements at central states. The phases of each current excitation feed point of the PAA are presented in Table 1

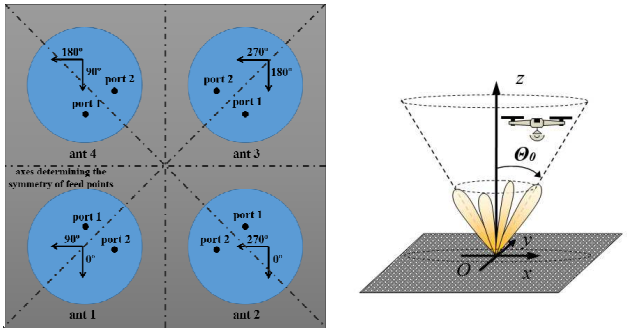

Fig. 2- The Phased antenna array model and basic scheme of work

The feeding network is created of a set of planar realized elements - Figure 3. The RP scanning is performed using delay lines (DL). They switch short lines with long lines, with an electrical length equal to the required phase to make RP necessary deviation - obtained in by using the equal (3), (4), and (5). The length of the DL is determined by [17]:

$$L_{dl} = L_{line} + \theta \qquad (6)$$

Where L_{dl} is the DL length, L_{line} - the extended microstrip line with θ. This is due to a change in the equivalent impedance when switching between a long and a short line takes place in the scanning process. To minimize these effects, the first device in the feed network is a Wilkinson power divider. Due to its topology, this hybrid divider is characterized by stability and wide bandwidth.

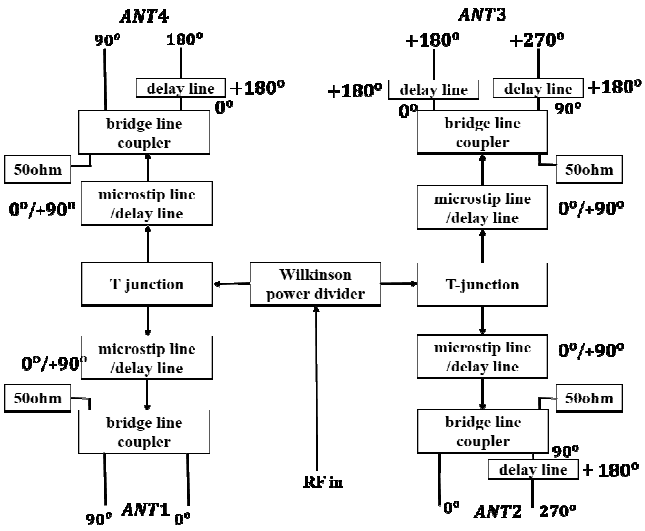

Fig. 3. The PAA feed network block diagram

TABLE I. CURRENT PHASE EXITAION FOR CENTRAL PAA RP STATE

patch element feed point	phase current exhibition
antenna 1, port 1	0°
antenna 1, port 2	90°
antenna 2, port 1	0°
antenna 2, port 2	270°
antenna 3, port 1	180°
antenna 3, port 2	270°
antenna 4, port 1	180°
antenna 4, port 2	90°

IV. SIMULATION AND MEASUREMENT RESULTS

The considered phased array antenna model is presented in Figure 4. Figures 5 ÷ 9 show a comparison results between simulation and measured RP. The radiation patterns measurement is performed through an autonomous measuring system discussed in [19], and measurements are made in open space, which minimizes interference effects. Table 2 gives measured RP for PAA design.

Fig.4a). PAA made model

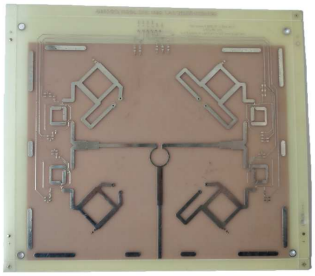

Fig.4b). Feed network realization

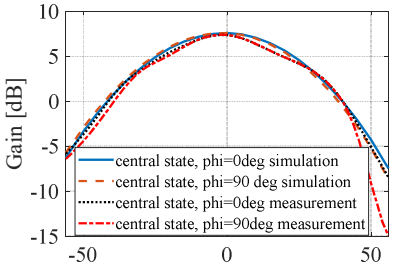

Figure 5. RP central state

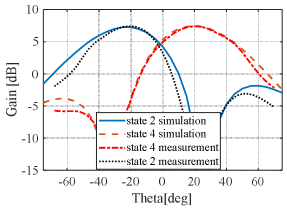

Fig. 6. RP –states 2 and 4

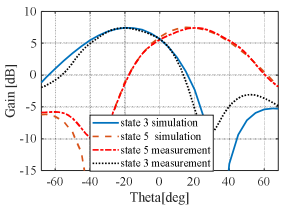

Fig. 7. RP –states 3 and 5

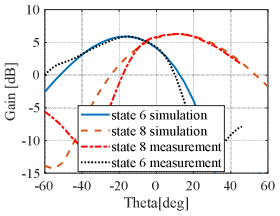

Fig. 8. RP –states 6 and 8

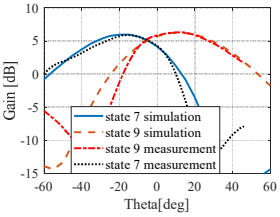

Fig. 9. RP –states 7 and 9

TABLE II. MEASURED RP FOR PAA DESIGN

Antenna RP states	Gain [Dbi]	RP beamwidth [deg]	Beam deviation [deg]
State 1	7.4	48º	-
State 2	7.4	47º	-20º
State 3	7.4	48º	20º
State 4	7.4	47º	-20º
State 5	7.4	48º	20º
State 6	6.2	46º	-16º
State 7	6.4	48º	15º
State 8	6.2	46º	-16º

Antenna reflection coefficient deviations are practically obtained when designing DL with RF switches (PE4259 are used) in the excitation network. Therefore, S11 parameters are not the same for the different RP states, but there nevertheless approximately equal. This ensures good operation of the center frequency antenna, with good bandwidth BW≥50MHz. The reflection coefficient for 2400MHz for the different states is presented in Table 3.

TABLE III. PHASED AANTENNA ARRAYS11 PARAMETERS

State	S11 [dB]
State 1	-21
State 2	-20.9
State 3	-21.2
State 4	-19.6
State 5	-23.7
State 6	-16.8
State 7	-15.8
State 8	-17.3

V. CONCLUSION

Thus designed circularly polarized phased antenna array with pseudo-conical scanning is fully applicable for integration into a pad for the unmanned landing of UAVs. The symmetry between the different radiation pattern states provides high accuracy in assigning the vehicle coordinates. In addition, the antenna is suitable for other radar purposes, as well as the incorporation in mobile communications of the latest generation, and automation of production processes and etc.

REFERENCES

[1] Maza, I., Caballero, F., Capitán, J., Martínez-de-Dios, J. R., & Ollero, A. (2011). Experimental results in multi-UAV coordination for disaster management and civil security applications. Journal of intelligent & robotic systems, 61(1), 563-585.

[2] Vallejo, David, et al. "Multi-agent architecture for information retrieval and intelligent monitoring by UAVs in known environments affected by catastrophes." Engineering Applications of Artificial Intelligence 87 (2020): 103243.

[3] Dimitrov, K., Damyanov, I., Saliev, D., & Valkovski, T. (2021, October). Pasture Research Using Aerial Photography and Photogrammetry. In 2021 29th National Conference with International Participation (TELECOM) (pp. 121-124). IEEE.

[4] Blistan, P., Kovanič, Ľ., Patera, M., & Hurčík, T. (2019). Evaluation quality parameters of DEM generated with low-cost UAV photogrammetry and Structure-from-Motion (SfM) approach for topographic surveying of small areas. Acta Montanistica Slovaca, 24(3).

[5] Bamburry, D. (2015). Drones: Designed for product delivery. Design Management Review, 26(1), 40-48.

[6] Witte, T. H., & Wilson, A. M. (2004). Accuracy of non-differential GPS for the determination of speed over ground. Journal of biomechanics, 37(12), 1891-1898.

[7] Andreev, K., & Stanchev, G. (2020). Flight safety sensor and auto-landing system of unmanned aerial system. International Journal of Reasoning-based Intelligent Systems, 12(3), 170-178.

[8] Fumio Ohtomo, Kazuki Osaragi, Tetsuji Anai, Hitoshi Otani, US Grant Patent number US20120277934A1, "Taking-Off And Landing Target Instrument And Automatic Taking-Off And Landing System", 2011

[9] Shen, X., Chang, R., & Yuan, D. (2019). Pseudo-monopulse tracking method for low profile mobile satellite antenna system. AEU-International Journal of Electronics and Communications, 101, 160-167.

[10] Nachev, I., & Iliev, I. (2020). A Simplified Design Methodology for Hybrid Antenna for S-band Application. Microwave Review, 26(2), 14-18.

[11] ung, Y. K., & Lee, B. (2011). Dual-band circularly polarized microstrip RFID reader antenna using metamaterial branch-line coupler. IEEE Transactions on Antennas and Propagation, 60(2), 786-791.

[12] M. Skolnik, "Radiolocation guide", 1976,

[13] Balanis, C. A. (2015). Antenna theory: analysis and design. John wiley & sons.

[14] Raj, J. S. K., & Schoebel, J. (2010). Designing antenna arrays using signal processing, image processing and optimization toolboxes of MATLAB. In MATLAB-Modelling, programming and simulation (pp. 261-276). Sciyo: InTech.

[15] Sahu, J. K., & Sethy, P. K. (2004). Design of linear, planar and circular antenna array using toolboxes of MATLAB. Trans. Pattern Anal. MachineIntell, 26(9), 1124-1137.

[16] Huang, J. (1986). A technique for an array to generate circular polarization with linearly polarized elements. IEEE Transactions on antennas and propagation, 34(9), 1113-1124.

[17] Nachev, I., & Petkov, P. Z. (2020, September). Radar Antenna Array Designing for Unmanned Aerial Vehicles (UAV). In 2020 55th International

[18] PE4259 datasheet available on https://www.psemi.com/pdf/datasheets/pe4259ds.pdf

[19] Iliev, I., & Nachev, I. (2020, September). An Automatic System for Antenna Radiation Pattern Measurement. In 2020 55th International Scientific Conference on Information, Communication and Energy Systems and Technologies (ICEST) (pp. 216-219). IEEE.